THE ZEUS EXPERIMENT AT HERA.

Proposal 760

Bristol, Glasgow, Imperial College London, University College London, Oxford, Rutherford Appleton Laboratory

in collaboration with

Andrews, Argonne, Bologna, Bonn, Calabria, Chonnan, Columbia, DESY, DESY-Zeuthen, Florence, Frascati, Freiburg, Hamburg, Iowa, Jülich, KEK, Krakow, Kyungpook, Madison (Wisconsin), Madrid, McGill, Moscow, NIKHEF, Ohio, Padova, Pennsylvania, Rome, Sagamihara, Santa Cruz, Seoul, Siegen, Tel Aviv, Tokyo, Tokyo Metropolitan Univ., Torino, Toronto, Warsaw, Weizmann Inst., Yale, Yokohama, York (Ontario).

1 Introduction

HERA continued to run in 2000 with positrons. The total luminosity delivered in 2000 was 66 pb^{-1} of which ZEUS wrote 51 pb^{-1} to tape. The ZEUS data-taking efficiency remained greater than 80%.

The ZEUS spokesman is a UK physicist and the UK provided the ZEUS tracking coordinator, the CTD coordinator, joint coordinators for three of the five physics groups and the ZEUS Monte Carlo code manager. The UK groups continued to take a large share of the responsibility in data-taking, yet again providing two of the four run coordinators in 2000, as well as a good proportion of the shift leaders and deputy shift leaders.

Currently the HERA accelerator is shutdown until late summer 2001 in order to upgrade the accelerator. During the shutdown ZEUS is taking the opportunity to upgrade the detector by installing a new microvertex detector, in which the UK have a signficant role, and a straw tube tracker. In addition the UK have a leading role in the upgrading of the polarisation measurement during the shutdown.

2 Central tracking detector status and infrastructure

The Central Tracking Detector (CTD) is a large volume cylindrical drift chamber covering the central region ($15^\circ < \theta < 164^\circ$). It provides charged particle tracking, momentum measurement and identification through dE/dx. It also participates in all three levels of the ZEUS trigger.

The CTD's 4608 sense wires are arranged in nine superlayers; superlayer one being the innermost. The wires in odd-numbered superlayers run parallel to the chamber axis, whilst those in the even-numbered layers have a small stereo angle ($\approx 5^\circ$). Taken together they provide sufficient information to reconstruct tracks in three dimensions. All wires in the chamber are equipped with Flash Analogue-to-Digital Conversion (FADC) electronics and, in addition, all wires in superlayer one and the odd numbered wires in superlayers three and five have z-by-timing readout for the first-level trigger.

The CTD readout has performed very reliably over the last year. Dead channels remain at no more than 2%. The chamber resolution and efficiency have remained stable for the last six years. We are confident that the chamber readout electronics will continue to perform reliably throughout the high luminosity running period after the HERA upgrade.

2.1 Triggering

ZEUS operates a three-level trigger, of which the first level is a hardware-based system whose principal aim is to reduce backgrounds that do not come from the interaction point. CTD information is essential for this and the detector uses dedicated, pipelined processor cards which provide tracking data to the global first-level trigger. The CTD first-level trigger has operated reliably throughout the last two years. As part of our ongoing maintainance program we are consolidating the test systems for the CTD first-level trigger electronics at the Rutherford Lab.

The ZEUS global second-level trigger uses more precise software algorithms to clean the event sample further and classify certain classes of physics events. Detailed tracking information is provided by the CTD second-level trigger which makes use of the data from all five axial superlayers and the z-by-timing information from layers 1, 3 and 5. A precise measurement of the event vertex at the second level is a powerful technique for rejection of background. In preparation for the HERA upgrade and the forthcoming microvertex detector, modifications have been made to the CTD transputer network to allow data from the FADC electronics to be sent to the proposed Global Tracking Trigger. This system will combine CTD data with the very precise tracking information from the microvertex detector, allowing a very accurate event vertex measurement with the possibility to tag long-lived particles.

The third-level trigger (TLT) runs on Unix workstations using an appropriate version of the off-line reconstruction code. The CTD TLT code is an optimised version of the full off-line reconstruction. Its performance is only slightly below that of the off-line version and aids monitoring of the system by providing early warning of any changes in critical CTD parameters.

2.2 Infrastructure, Slow Control and Monitoring

The advent of the year 2000 necessitated some changes to the CTD online computer systems. At the end of 1999 the old VAX-VMS computers used for the CTD run-control and monitoring systems were replaced with new AXP-OpenVMS workstations that are fully Y2K compliant. The new systems have operated continuously since their installation without problems.

Online data-quality monitoring (DQM) is an important issue. ZEUS has adopted an approach whereby simple DQM checks are performed automatically and the shiftcrew notified if any problems are found. The CTD DQM system is, therefore, being updated to work in this new framework. More detailed, off-line DQM checks are still performed by the automatic job-submission system that has been used for the last few years. This system has proven to be most effective, both in terms of efficient utilisation of manpower and timely diagnosis of problems on the chamber.

In general the support infrastructure for the CTD has performed well. There have been two incidents connected with the chamber cooling system where the narrow water pipes clogged with copper residue. The first incident was solved by reversing the water flow though the cooling pipe, flushing out the blockage. However, since the pressure of the cooling water supply to the CTD was reduced in 1999 there has been an increased tendency for the pipes to block. To remedy this a new booster pump has been purchased in collaboration with the DESY cooling water group. This pump has now been installed in the CTD cooling circuit and it is hoped that, in conjunction with a set of fine filters, this will solve the problem.

The continued operation and reliability of the CTD is of utmost importance to ZEUS. The CTD has operated reliably without causing any significant down-time for the experiment for almost ten years. However, during 2000 there were many instances of repeated trips of the high voltage (HV) in the outer superlayers. The only way to recover the affected parts of the chamber was to disable the HV to that region for typically a few days before attempting to switch it on again. It should be stressed that the problems to date have been confined to superlayers eight and nine which play no part in the first-level trigger. The impact on the second- and third-level

triggers is small. Extensive investigations failed to show any correlation between the frequency of the trips and external environmental factors - including gas composition. The conclusion was that the cathode wires in the chamber were becoming coated with some insulating material (the "Malter" effect [9]), which causes the HV problem. To address this possibility, the CTD gas system was modified to allow water to be added to the gas mix. After adding water to the gas no further trips were observed. We have concluded that the problem has now been successfully addressed and will continue to run with water in the gas for the remaining lifetime of the experiment.

3 ZEUS Microvertex Detector

ZEUS UK groups at RAL, Oxford and UCL were originally involved in 3 aspects of the ZEUS microvertex detector (MVD) project: the clock and control electronics; online and offline alignment and installation. Recently Glasgow has joined the offline alignment effort. For strong physics reasons and because of the experience of the UK groups in track triggers, we continue to give some support to the development of a global track trigger (GTT) which will eventually use hits from the MVD, CTD and forward trackers. This work, as well as our involvement in the off-detector electronics, is closely connected to the DAQ and slow control systems. As part of this effort, an integrated online event display and histogram presenter for MVD hits has been produced. Through discussions on installation procedures we now have responsibility for a cable patch box which has grown into a larger and more expensive task than anticipated. Because of a severe shortage of effort at RAL, UCL and Oxford had to take on more responsibility in the areas of clock and control and installation respectively. Before discussing the UK tasks in more detail a brief overview of the detector and project status is given.

The MVD consists of a central barrel section with 3 layers (over most of the solid angle; 2 elsewhere) of silicon microstrip detectors and 4 forward wheels. Each layer provides readout in two coordinates, using two layers of microstrip detectors with readout pitch at right-angles. The barrel has a total of 600 individual detectors arranged on 30 ladders running parallel to the beam pipe. The wheels contain a total of 112 sensors. The silicon detectors are read out using the HELIX chip mounted adjacent to the detectors, a total of 1648 chips for the 20736 channels. The key design parameters of the MVD are: angular coverage $10^\circ - 170^\circ$; impact parameter resolution of $100\,\mu$m at 90°; two-track separation of $200\,\mu$m. The active planes of the vertex detector are mounted in a carbon fibre tube 2m long supported from the ends of the CTD. The beampipe has a central section of Al-Be welded to forward and rear conical sections made of Al. The beampipe is not attached to the MVD. The total material in the barrel region is $8\%X_0$ of which 82% is from the silicon ladders and on-board electronics.

Assembly of the MVD has been in full swing at NIKHEF and DESY since the late summer 2000. The upper half of the detector was transported to DESY in mid-December where it is now being prepared for 'full system tests' (in the tent in the old JADE Hall in which the CTD was prepared for installation). The bottom half will follow in early February 2001 and installation in ZEUS of the complete MVD will take place in late March/early April.

3.1 Clock and Control Electronics

The clock and control (C+C) system for the MVD distributes the HERA clock and the ZEUS first level triggers to the HELIX readout chips. It also contains logic to handle error conditions and busy signals from the GFLT and the MVD ADC system, and distributes calibration data from the slow control at the beginning of a run. The original proposal envisaged a split system with a "Masterbox" and "Slaves" positioned in the rucksack adjacent to the ADCs, dealing with the digital logic, and a "HELIX driver" system positioned close to the detector fanning out the

signals from the masterbox and dealing with the calibration data. The masterbox system and the HELIX driver are the responsibility of UCL.

The Masterbox and Slave design remain largely unchanged, although the systems are now positioned closer to the detector than originally envisaged, but further from the GFLT. This change was motivated by space requirements and the need to place the ADCs closer to the detector, and implied significant changes to the cabling scheme. The masterbox was successfully prototyped and the final master and slave system has now been built, tested at UCL and delivered to DESY.

The HELIX driver has undergone substantial design modifications, principally driven by the need to drive the HELIX chips from 5m from the detector rather than the 10-20m originally intended. The fanout from the masterbox to 200 modules is still performed on a HELIX driver board which also interfaces with the slow control for calibration. This part of the clock and control remains largely unchanged from the original design, although it now sits about 24m from the detector, adjacent to the masterbox and ADCs. However, because of the difficulty in driving the CMOS signals to the HELIX chips, a current amplifier is required in a patch box.

3.2 ZEUS MVD Optical Alignment

The purpose of the optical alignment system is to provide measurements of the position of the MVD support structure with respect to the CTD with precision of 20 μm or better. The detailed alignment of the individual silicon wafers will be performed using the conventional method using tracks of charged particles. The alignment system will also measure distortions of the structure as a function of time, thus defining stable periods for the alignment procedure using tracks.

The MVD consists of a tube made of two half cylinders. The optical alignment system was installed in both half cylinders before the main assembly started. A test to measure stability of the alignment system was performed in Aug. 2000 for two weeks. The system was stable except for an initial relaxation of mechanical stress. During assembly period and after the transportation of one half cylinder, the system measured the position of each support structure with respect to reference points. The result suggests sag and small rotation of the half cylinder during the assembly period due to the added weight to the structure. No significant change was observed due to the transportation. The same measurement will be repeated for the other half cylinder. The system worked very well and demonstrated the deformation of one half cylinder during assembly. An interface to control laser delivery system is being designed for the final system. A prototype of a VME read-out module for the final system was built and is being tested.

3.3 Track Trigger and MVD DAQ

Because of the large degree of expertise the ZEUS UK groups have with track triggers, we contribute to the work on possible improvements to ZEUS track triggering after the upgrade, but do not have sufficient resources to take full responsibility for any new trigger. As part of this contribution, we have made the FADC information currently sent to the existing CTD second level trigger (SLT) also available to a new trigger by the addition, in 1999, of extra transputer links to the readout and SLT transputer network.

With the enormous increase in processing power of computers over the past 10 years – particularly commodity PC's – it is now possible to perform on a single PC what then required sophisticated parallel processing. We have continued to provide effort for the development of a new global track trigger (GTT). This trigger is forseen to run on a farm of 10 dual processor 1GHz Linux PC's provided by Intel, each processor completely handling the tracking from the CTD, MVD and the new forward Straw Tube Tracker (STT) for a single event. The project also offers excellent training opportunities for graduate students and currently includes from the

UK one UCL student and one Post Doctoral Research Associate from Oxford, both working part-time.

Progress so far has been encouraging, and has included a port of the existing CTD SLT algorithm from OCCAM (the transputer language) to C. In addition, the algorithm has been extended to include MVD hit information and CTD stereo wire information in place of that from the z-by-timing system. Data transfer rate studies have been performed using a transputer to VME interface (originally designed by NIKHEF for the ZEUS global second level trigger) and a network of PowerPC's (the hardware provided by the ZEUS DESY group). Additionally algorithm perfomance studies have begun – figure 1 shows the improved z-vertex resolution using CTD stereo and ideal MVD data. The results are very encouraging and it has been demonstrated that the single cpu algorithm with axial plus stereo data has a mean latency of less than 1 ms on a 750 MHz Pentium III PC, compared to $\sim 10 - 12$ ms for the present system. Work has now started on integrating the algorithm into the PC farm and the MVD DAQ system for use in the MVD system tests.

Although originally intended to provide the online software for the clock and control system, it turns out to be more efficient for this to be provided in the framework of the DESY-led MVD DAQ team. Instead, as part of this team, UCL has provided an online histogramming and event display package for the MVD. This ties in well with our alignment and trigger activities and will be an invaluable tool during the system tests prior to installation, and during the first months of data taking at the newly upgraded HERA collider.

4 The HERA Polarimeter Upgrade

4.1 Overview

The determination of the cross sections for CC and NC DIS at high Q^2 using polarised electron and positron beams is of first importance in detailed studies of the Standard Model, SM. At present there are no measurements of charged current (CC) deep inelastic scattering (DIS) using polarised charged lepton beams and the data on the polarisation dependence of neutral current (NC) DIS is limited to low Q^2. These measurements will be one of the primary objectives of the ZEUS collaboration after the HERA upgrade. The polarisation dependence of the NC and CC cross sections is a direct consequence of the chiral structure of the SM, hence, measurements of these cross sections will allow important tests of the electroweak (EW) sector of the SM to be made [2]. Two key examples of such tests are highlighted below.

1. Search for Right-Handed Charged Currents:
   A comparison will be made of the cross section for CC scattering using left- and right-handed beams. This will allow the chirality of the CC weak interaction to be observed for the first time using charged lepton beams and as such will represent a significant test of the Standard Model. For example, in one year's running, a model independent limit on the mass of a hypothetical boson, W_R, mediating CC reactions between right handed fermions can be set at the level of ~ 400 GeV.

2. Measurement of the Light Quark Couplings to the Z-boson:
   The full potential of electroweak measurements at HERA will be realised when data have been taken with each of the four charge/polarisation combinations. It is by detailed comparison of the polarised NC and CC cross sections that the couplings of the u- and d-quarks to the Z-boson can be extracted. For example, with 250 pb^{-1} per charge/polarisation combination the u-quark couplings to the Z-boson can be measured with a precision of 10%.

These measurements require that the polarisation be known with a precision of 1 - 2%. The present polarimetry at DESY yields a precision of only ~4%, making an upgrade of the system

essential [3].

At present the HERA polarimetry system consists of two polarimeters [4]. The first, the transverse polarimeter, TPOL, is located in the HERA West area. The second, the longitudinal polarimeter, LPOL, is situated in the HERA East area upstream of the HERMES experiment where a pair of spin rotators are installed. The spin rotators rotate the natural transverse polarisation of the electron or positron beam into longitudinal polarisation.

Both the TPOL and the LPOL employ a laser to provide a beam of circularly polarised light which is shone upon the lepton beam. The degree of polarisation may now be determined by detecting Compton photons back-scattered off the lepton beam. The principle of operation of the devices is different. The transverse polarisation is best determined by measuring the spatial, up-down, asymmetry of the back scattered photon, while the longitudinal polarisation is determined by measuring the energy asymmetry of the photons. The two photon detectors, therefore, are optimized to measure the spatial coordinate of a photon in the case of TPOL, or the energy of a photon in the case of LPOL. Both detectors exist and have been operating for a number of years.

The TPOL calorimeter is separated horizontally into two halves. The energy sharing between the upper and lower halves may be used to determine the impact position of a photon in the vertical direction. The up-down position asymmetry used to determine the polarisation relies on the conversion of the up-down energy asymmetry into a vertical position. This conversion is referred to as the '$\eta(y)$-transformation'. At present the uncertainty on the $\eta(y)$-transformation gives the largest contribution to the systematic error on the measurement of the transverse polarisation. A precise determination of the $\eta(y)$-transformation in situ during running will lead to a significant improvement in the precision of the measurement of the transverse polarisation. In order to determine the transformation precisely it has been proposed to install a pre-radiator, instrumented with a silicon micro-strip detector, in front of the TPOL calorimeter.

We are currently engaged in the commissioning and evaluation of a silicon microstrip prototype system. The prototype front-end board comprises a 1×1 cm^2 single-sided silicon strip detector with a pitch of 80 μm. The detector is read out with an APV25 amplifier/multiplexer chip [5]. The prototype front-end board, designed and built at Imperial College, has been operated successfully in a test stand controlled with a Macintosh computer running LabView. A VME based readout system for the prototype, has been developed and tested at Imperial College. In August 2000 the silicon microstrip prototype system was installed in the HERA tunnel in the TPOL area at DESY, to test the system in the real photon Compton beam and HERA environment. Proper test beam studies will be carried out at DESY and CERN in the first months of 2001.

4.1.1 Silicon Detector and Readout

In order to achieve the required relative precision on the transverse polarisation a pre-shower detector with position resolution of ~ 30 μm is required. The position detector will also allow the calorimeter to be centred precisely on the Compton photon beam. The position detector must work in a region of very high photon flux. We therefore propose to use radiation-tolerant silicon for both the detector and the front-end readout electronics. The detector will be a 5×5 cm^2 single-sided silicon microstrip detector with a strip pitch of 80 μm. We will read the detector out with five APV25 chips. The front-end readout will be controlled using a VME system via an I2C interface board and the clock and control signals will be generated using a suitably modified SEQSI board [6, 7].

4.1.2 Precision Mechanical Support Structure

The silicon detector must be precisely positioned with respect to the calorimeter. In addition, we require a method by which the linearity of the position response can be calibrated at the level of 10 μm or better. We are currently considering how best to perform this calibration. It has been shown that the linearity of the response of the position detector can be achieved using a scintillating fibre. The fibre would be supported horizontally in front of silicon detector and moved in the vertical plane by means of a precision stage. Work at Imperial College is progressing in constructing the mechanical parts of this assembly. The calibration system (scintillating fibre, photo-detectors, readout and associated software) will be the responsibility of other ZEUS members of the POL2000 collaboration.

5 Physics analyses

During 2000 17 ZEUS analyses were published or submitted for publication ([12]-[28]) by various journals, of which 8 were originally submitted in 1999. In this section, we concentrate as usual on those physics areas where the UK members of ZEUS have been particularly active.

5.1 High Q^2 Neutral, Charged Current Physics and Structure Function Measurements

5.1.1 High Q^2 Neutral Current Physics

In Deep Inelastic Neutral Current (NC) scattering, a photon or a Z_0 may be exchanged between the incoming lepton and the proton. The cross section for Deep Inelastic NC scattering is given below.

$$\frac{d^2\sigma^{\pm}}{dxdQ^2} = \frac{2\pi\alpha^2}{xQ^4}[Y_+F_2(x,Q^2) - y^2F_L(x,Q^2) \mp Y_-xF_3(x,Q^2)] \quad (1)$$

where $Y_{\pm} = 1 \pm (1-y)^2$ and the structure function F_2 can be decomposed into $F_2 = F_2^{EM} + F_2^{Weak} + F_2^{Int}$, where F_2^{EM} represents the contribution from γ-exchange, F_2^{Weak}, the contribution from Z^0 exchange, and F_2^{Int} the contribution from $\gamma - Z^0$ interference. The parity violating cross-section xF_3, becomes significant at large x and Q^2.

ZEUS UK physicists have continued their leading role in studies of high Q^2 physics at HERA. In August 1998 HERA switched to running with electrons until the end of May 1999, delivering a luminosity of 16 pb^{-1}. This allows for the first time a high statistics measurement of the $e^- p$ high Q^2 Deep Inelastic scattering Neutral Current cross sections. This permits the first comparison of the charge dependence of the NC cross section at high Q^2, showing the sensitivity to the contribution of Z^0 exchange. Figure 2 shows the neutral current differential cross section $d\sigma/dQ^2$ as a function of Q^2 for both electron and positron beams, also compared are the predictions from the standard model using CTEQ4D parton densities. In figure 3 $d\sigma/dx$ for $Q^2 > 10\,000\,\mathrm{GeV}^2$. The effect of the positive interference of the photon γ and Z^0 can be clearly seen in the electron data from figure 3.

A measurement of the double differential reduced cross section $\tilde{\sigma}$ is shown in figure 4, the reduced cross section is described below.

$$\tilde{\sigma}_{NC}(x,Q^2) = \frac{1}{Y_+}\frac{xQ^4}{2\pi\alpha^2}\frac{d^2\sigma_{NC}}{dxdQ^2} \quad (2)$$

The data are seen to be well described by the Standard Model predictions from CTEQ4D and MRST [30] Shown in figure 4 is the reduced cross section at fixed x as a function of Q^2 for both the e^-p and e^+p data sets. For Q^2 values above $1000\,\mathrm{GeV}^2$ the e^-p reduced cross section is clearly seen to turn upwards, where the e^+p data is seen to turn down. This is consistent with

the Standard Model expectation in which one expects positive interference of the Z_0 exchange for e^-p scattering and negative interference for e^+p scattering.

The new high statistics electron data in combination with previous and forth coming positron data allows the first extraction of the proton structure function xF_3 at high Q^2 and x. The extraction of the parity violating structure function xF_3 is achieved from the following method. The data sets used for the extraction of xF_3 are $30\,\mathrm{pb}^{-1}$ of e^+p data taken in 1996/97 and the $16\,\mathrm{pb}^{-1}$ of e^-p data taken in 1998/99.

The extraction of xF_3 is shown in figure 5. This shows the measured xF_3 in bins of Q^2 as a function of the scaling variable x compared with the Standard Model expectations from CTEQ4D and MRST. It can be seen from that the Standard Model predictions are in good agreement with the data. The shaded band shows the correction of F_l to the expected value of xF_3 scaled by a factor of 10.

The precision of the xF_3 measurement is comparable with the first extraction of F_2 from data taken in 1992. This measurement will clearly benefit from an increased data sample from the HERA luminosity upgrade. An improved measurement of xF_3 allows a better constraint on the high x valence quark distribution, which will play an important role in estimating very high energy processes at the LHC.

5.1.2 High Q^2 Charged Current Physics

In Charged Current (CC) deep inelastic scattering (DIS) the exchanged W-boson picks out specific quark flavours from within the proton. Thus e^+p CC DIS is sensitive to the d valence quark density at high x and the $\bar{u}$ (and $\bar{c}$) quark density at low x. By contrast, e^-p CC DIS is sensitive to the u valence quark density at high x and the $\bar{d}$ (and $\bar{s}$) quark density at low x. Hence by measuring the dependence of the CC DIS cross section on the charge of the lepton beam we are able to study flavour-specific parton densities directly.

In 1999 ZEUS published measurements of the single and double differential e^+p CC DIS cross sections based on 48 pb^{-1} of data taken during the years 1994-1997 [29]. The publication also contains a determination of the mass of the W boson, M_W, using the PDG G_F value. A fit to the measured differential cross section $d\sigma/dQ^2$, treating M_W and G_F as free parameters was also performed in order to investigate the extent to which the SM gives a consistent description of the data. The value of M_W obtained agrees with the value of $M_W = 80.41 \pm 0.10$ GeV from the PDG fit, using time-like production of W-bosons at the Tevatron and at LEP. Since CC DIS represents space-like exchange, the result is complementary to measurements of M_W from $p\bar{p}$ or e^+e^- annihilation and constitutes an important check of SM consistency.

The analysis of the 16 pb^{-1} of e^-p data taken during 1998 and 1999 with a proton beam energy of 920 GeV is now approaching conclusion. Preliminary results from the full data set, and for $Q^2 > 200\mathrm{GeV}$ were shown at the summer conferences of 2000. Figure 6 shows the cross section $d\sigma/dQ^2$ for e^-p scattering. The SM expectations, evaluated with the CTEQ5D and MRST(99) PDFs, give a good description of the data. The double differential CC cross section may be written as

$$\frac{d^2\sigma^{CC}}{dx\,dQ^2} = \frac{G_F^2}{2\pi x}\left(\frac{M_W^2}{M_W^2+Q^2}\right)^2 \tilde{\sigma}$$

where the e^-p reduced cross section, $\tilde{\sigma}$, is given at leading order by $\tilde{\sigma} = u + c + (1-y)^2(\bar{d}+\bar{s})$ (for e^+p change quarks to anti-quarks and vice versa). The reduced cross section, for both e^-p and e^+p, is plotted as a function of x at several fixed values of Q^2 in figure 7. The e^-p cross section is everywhere higher than that of e^+p, rising to a factor 10 at the highest Q^2 measured. In the quark parton model, this is understood to be due to the W coupling to the higher u-quark density in e^-p scattering, while the dominant e^+p process is the W coupling to d-quarks with

a $(1-y)^2$ suppression. The Standard Model (SM), evaluated with the CTEQ5D PDFs, gives a good description of the data,

The analysis of the recent e^+p data taken with a proton beam energy of 920 GeV is well underway. All the data taken up to September 2000 will be combined to give the definitive $e^{\pm}p$ CC DIS cross sections from ZEUS using unpolarised lepton beams.

5.1.3 Structure Functions

ZEUS UK groups continue to be strongly involved in the measurement and analysis of structure functions and provided a physics group coordinator in this area during 2000. The groups were also well represented in the relevant working groups at the DIS2000 Conference in Liverpoool. UK people took the lead in drawing together various phenomenological approaches to ZEUS F_2 data over the full range of Q^2 [10]. The impact of the 1994 ZEUS data on NLO DGLAP fits, including a full treatment of systematic errors, was examined with particular emphasis on the low x low Q^2 region. This was part of a wider study of the transition region from pQCD to soft physics as $Q^2 \to 0$. The paper includes plots of the two slopes $dF_2/d\ln Q^2$ ('Caldwell' plot) and $dF_2/d\ln(1/x)$ that are important in the study of the transition region. Figure 8 shows the singlet and gluon momentum distributions from the NLO fits as functions of x in different Q^2 bins. The figure shows the importance of the F_2 data at low x and Q^2 in reducing the error on the gluon distribution at low x. It also shows that at the lowest Q^2 ($1\,\mathrm{GeV}^2$) the gluon density is probably less than that of the sea quark, provided that the DGLAP approach is still valid. This result is not what one would expect from a conventional understanding of the QCD enhanced parton model and may indicate that contributions beyond DGLAP are becoming important. We continue to work on the extraction of the very high statistics F_2 data set from the HERA 1996/7 runs. This data will be the definitive measurement at low and medium Q^2 by the ZEUS experiment. It is hoped that the data will be published later this year. We are also involved in NLO QCD fitting of the data and other phenomenological analyses.

5.2 Charm and Beauty Production

5.2.1 Charm Production in DIS

Heavy flavours, particularly charm, are produced copiously in DIS at the low x values available at HERA. The dominant production mechanism is the boson-gluon fusion (BGF) process, which in principle means that this channel offers another way of measuring the gluon density in the proton. Charm is identified by the decay chain $D^* \to D^0\pi^+$, $D^0 \to K^-\pi^+$ or $D^0 \to K^-\pi^-\pi^+\pi^+$ and as the combined branching ratios in the D^* and D decays are only a few percent, the measurement requires a large luminosity. Since the threshold region is explored at low Q^2 it is necessary to use the massive quark BGF formalism, which has been worked out to NLO. UK groups were involved with the recent ZEUS measurement of F_2^c using the 1996 and 1997 data with a combined luminosity of $37\,\mathrm{pb}^{-1}$ [12]. Totals of 2064 ± 72 and 1277 ± 124 events were found for the $K\pi$ and $K3\pi$ decay channels respectively, representing an order of magnitude increase over earlier measurements at HERA. Figure 9 shows F_2^c as a function of x in bins of Q^2. The steep rise at low x at Q^2 above $4\,\mathrm{GeV}^2$, seen in the full F_2 data, is very striking. The curves show the expectation of the NLO BGF process, with the gluon distribution from the ZEUS QCD fit referred to above and with $m_c = 1.4\,\mathrm{GeV}$. The largest contribution to the uncertainty shown for the calculation is from the uncertainty in charm mass, here a variation of ± 0.2GeV was allowed. High statistics measurement of heavy flavour processes will be a major goal with the MVD after the upgrade.

5.2.2 Charm Production in Diffractive Scattering

The measurement of charm production in diffraction is crucial to the understanding of the underlying mechanism of diffraction. The various models of diffraction predict significantly different behaviour for gluons. As charm production predominantly occurs in gluon-driven interactions, it is clear that the predictions for charm production in diffraction will also vary significantly from model to model.

UK physicists are the principal contributors to the analysis of diffractive charm production in DIS, which is being performed using the 1995-1997 dataset (44 pb^{-1}). As in the analysis of non-diffractive charm production, charm is tagged through the reconstruction of charged $D^{\star}$ mesons using two different decay channels. The analyses of both decay channels are well advanced and a paper draft is almost ready for consideration by the Collaboration. It is expected that this paper will be prepared for publication this year. These studies will benefit greatly from the improved statistics and better non-diffractive background rejection expected after the upgrade.

5.2.3 Charm and Beauty Photoproduction

Charm quarks inside jets were measured via D^* decays at ZEUS in 1998 and published in 1999 [11], with UK physicists as principal authors. The results showed for the first time that charm is produced copiously in resolved photon events.

Heavy quarks can also be detected by identifying electrons from their decay. This is done by measuring the distinctive rate of energy loss of electrons in the CTD, as well as the way they interact in the calorimeter. Results by UK physicists from this method not only confirm the result of the D^* studies, but also show a significant production rate for beauty quarks as may be seen in figure 10. The beauty component is identified by measuring the transverse momentum of the electron relative to the jet axis since electrons from beauty decays are expected to have a harder p_t^{rel} spectrum owing to the mass of the b. The beauty fraction has been extracted by fitting the data distribution with Monte Carlo. Using this fraction the visible cross section can be compared to LO QCD models [28].

Existing measurements of open beauty production from both HERA and $p\bar{p}$ colliders show cross sections that are high when compared to standard NLO QCD predictions. A direct comparison of the ZEUS result with an NLO QCD prediction is also possible by using the Monte Carlo to extrapolate to the $b\bar{b}$ cross section in a limited kinematic region. This extrapolated cross section also lies above the theoretical prediction.

Understanding such results is an important test of QCD and a necessary step towards understanding the new physics potential of future colliders. The results also represent a substantial technical triumph in the operation and understanding of the CTD dE/dx readout, a UK responsibility from the beginning of ZEUS.

The presence of heavy quarks in the evolution of the photon structure offers a promising window for understanding the development of QCD structure, splitting functions and threshold effects. The ability at HERA to select concurrently on E_T^{jet}, photon virtuality and x_γ^{OBS}, as well as to compare heavy flavour jets with untagged jets, makes it uniquely suitable for detailed studies in this area. Thus heavy flavour jet production will be a growth area, and is a major driving force behind the UK's involvement in the MVD. The GTT will play a vital part in allowing these events to be saved at relatively low E_T^{jet} even after the upgrade, particularly if charm enrichment can be implemented.

5.3 Jet Production

Our studies of jets in photon-proton collisions at HERA continue to give information on the hadronic "structure" of the photon, and UK groups continue to lead these analyses. Since

the last report we have measured [31] the dynamics of three jet production with higher statistics than our previous measurement [32] and shown explicitly the effects of the colour of the incoming quarks and gluons (see figure 11) which is a fundamental test of the strong interaction. We have also measured the dijet angular distributions with high statistics and at high E_T^{jet}.

Although these studies present a reassuring picture of jet photoproduction in that the dynamics are well described by QCD, there is clear and growing evidence for a significant discrepancy in the rate of resolved photon interactions, with the data lying above the NLO QCD expectations by around 30%. We have measured cross sections differential in η^{jet}, E_T^{jet} and x_γ^{OBS}, the fraction of the photon's momentum entering the hard subprocess. In all cases, although the direct-photon dominated high x_γ^{OBS} region agrees well with the theory, the resolved-photon dominated low-x_γ^{OBS} region shows an excess as may be seen in figure 12. The current evidence points to the photon structure as the source of this discrepancy. ZEUS is sensitive to the photon structure in a Q^2 region not measured by LEP. We are continuing work on reducing the systematic uncertainties in the measurements and evaluating the implications for photon structure and QCD.

5.4 Azimuthal Asymmetries

In DIS, the distribution of the azimuthal angle, ϕ, (measured in the hadronic centre-of-mass frame) between the lepton scattering plane, defined by the incoming and outgoing lepton momenta, and the hadron production plane, defined by the incoming virtual boson and an outgoing hadron has been measured.

Figure 13 shows the distributions of the azimuthal angle of the leading hadrons. The four plots are made with increasing minimum transverse momentum, p_c, of the hadrons. It can be clearly seen that at higher p_c the events follow a $\cos 2\phi$ distribution. This is a clear prediction of perturbative QCD which has never before been observed.

5.5 Event Shapes

A recent revival of interest in the study of event shape measurements has been prompted by theoretical developments in the understanding of hadronisation or power corrections. Here, perturbative QCD calculations are extended into the region of low momentum transfers using approximations to higher-order graphs. At HERA, the Q^2 scale can be varied over four orders of magnitude enabling power corrections (proportional to $1/Q^p$, where p is the power) to be studied in detail. The data are compared to theoretical expectations for the power corrections, characterised by an effective coupling $\overline{\alpha}_0(\mu_I)$ specified at the infra-red matching scale $\mu_I \simeq 2$ GeV, and NLO pQCD calculations, determined by $\alpha_s(M_Z)$.

The Breit frame is where the exchanged gauge boson in DIS is purely space-like. Viewed in this frame, the incoming QPM quark is back-scattered with equal and opposite momentum $(Q/2)$. Event shapes have been measured in the direction of the struck quark, corresponding to the current region, which is directly analogous to one hemisphere of a purely time-like e^+e^- interaction. A series of event shape variables have been studied which have varying sensitivity to hadronisation/power corrections and are noted below. Thrust ($\tau = 1 - T_z$) and jet broadening (B) sum the longitudinal and transverse momenta, respectively, of individual particles along the photon axis. τ_c is also defined with respect to the reconstructed thrust axis, in order to compare directly with e^+e^-. Jet mass (ρ) and the C parameter sum the product of two particle momenta weighted by $1-\cos\theta_{ij}$ and $\sin^2\theta_{ij}$, respectively. These variables are each measured in the current region of the Breit frame and are scaled by the total visible energy (E_{vis}).

Mean values of these event shapes haves been measured by ZEUS [33] which can be interpreted theoretically via

$$\langle F \rangle = \langle F \rangle^{\rm pert} + \langle F \rangle^{\rm pow}$$

where

$$\langle F \rangle^{\rm pert} = c_{1,F}(x,Q) \cdot \alpha_s(Q) + c_{2,F}(x,Q) \cdot \alpha_s^2(Q)$$

with $c_{1,F}(x,Q)$ and $c_{2,F}(x,Q)$ being calculable coefficients of pQCD determined by the DISENT NLO program with renormalisation/factorisation scales set at $\mu_R = \mu_F = Q$. The power corrections are proportional to $1/Q$ with

$$\langle F \rangle^{\rm pow} = \mathcal{M}' \frac{a_F}{Q} \frac{16\mu_I}{3\pi} \left[\overline{\alpha}_0(\mu_I) - \alpha_s(Q) - \frac{23}{6\pi} \left(\ln \frac{Q}{\mu_I} + 1.45 \right) \alpha_s^2(Q) \right].$$

Here a_F is a calculable F-dependent coefficient and $\mathcal{M}' = 2\mathcal{M}/\pi \simeq 0.95$ is a two-loop level refinement to the calculations called the Milan factor.

The measured mean event shape values versus Q are shown in Figure 14, where the data are compared to two-parameter fits in $\overline{\alpha}_0(\mu_I)$ and $\alpha_s(M_Z)$ using the NLO calculation plus power correction approach described above. Overall, a reasonable description of the data can be achieved, although the x-dependence of variables measured with respect to the photon axis, τ and B, is not well described. The major theoretical uncertainty is that due to the renormalisation scale, indicated by the shaded band.

The results of two-parameter fits to the ZEUS data are given in Figure 15. The correlation of $\overline{\alpha}_0(\mu_I)$ and $\alpha_s(M_Z)$ is high and negative for $\langle \tau \rangle$ but is less for other variables. In each case, the data for the means of τ, B, τ_C, C and ρ, are described reasonably well by the theory, with a value of the universal non-perturbative parameter $\overline{\alpha}_0(\mu_I)$ of $\simeq 0.5 \pm 20\%$ and a value of $\alpha_s(M_Z)$ close to the world average. There are, however, remaining theoretical uncertainties due to uncalculated higher-order x-dependent terms which appear to be especially significant for B. In conclusion, the theoretical approach works remarkably well and ongoing refinements will generate further insight into non-perturbative QCD mechanisms in the generation of hadronic final states at high energies.

5.6 Inclusive Prompt Photon Photoproduction at HERA

A third ZEUS paper on prompt photon production is in the final stages of preparations for publication. In this analysis we study the effects of acollinearity between a prompt photon produced in photoproduction at ZEUS and the associated recoil jet. Projected into the r-phi plane, the mean transverse momentum of the photon relative to the jet direction is a measure of the mean transverse momentum of the initial-state quark as it is struck by the incoming photon. Traditionally, this quantity has been thought of as the 'intrinsic' quark momentum within the proton, governed by the confinement of the quark within the given radius of the proton. However the present measurement gives a larger value which appears to be influenced by higher order QCD effects in the initial-state parton shower associated with the hard scattering process (prompt photons and jets with transverse momentum of at least 5 GeV) are selected). The result is consistent with those from other experiments and invites further theoretical input. Figure 15 shows the effective transverse momentum of quarks within a proton, as they take part in direct photoproduction of a high transverse momentum prompt photon and a jet. Comparison is made with a variety of measurements from other experiments over a wide range of interaction energies W. A consistent trend is observed.

A start has been made on a further study of prompt photon production in Deep Inelastic Scattering processes.

5.7 High-Pt lepton analysis

Events with isolated high-energy leptons and missing transverse momentum are signature of $l\nu$ final state from single-W production, which has a small cross section of about 1 pb, followed by

its leptonic decay. The event topology is also an experimental signature for the production of new particles, such as scalar quarks in the framework of an R-parity-breaking SUSY model.

ZEUS experiment searched for this type of events using 1994–1999 data corresponding to an integrated luminosity of 82 pb^{-1}. The number of observed events, seven with $e^{\pm}$ and four with muons, is consistent with the 6.1±0.9 (3.7±0.4) electron-type (muon-type) events expected from Standard Model processes. The kinematic variables of the events lie in the region predicted by the Standard Model. The excess of such events reported by the H1 collaboration is therefore not confirmed by the ZEUS data.

6 UK Theses

(Submitted during 2000.)

1. O Ruske (Oxford, 2000) *Measurement and Phenomenology of the Proton Structure Function F_L using the 96/97 ZEUS data at HERA*, D.Phil Thesis Oxford, Oct. 2000
2. Sung Won Lee (Glasgow, 2000) *Measurements of Prompt Photon Photoproduction at HERA.*
3. J Scott (Bristol, 2000) *First Direct Measurement of F2 Using ISR Events in DIS at HERA.*
4. O Barret (Bristol, 2000) *Diffractive D* Production in Deep Inelastic ep Scattering at HERA.*

Talks on ZEUS and ZEUS-related physics given at major National or International Conferences.

1. R Walczak (Oxford), *Recent results from HERA*, 16TH Nordic meeting in particle physics 4-10 Jan 2000, Oslo, Norway: SPAATIND2000
2. R Walker (I.C.), *High Q^2 Charged and Neutral Current Results from HERA*, Moriond Conference on Electroweak Interactions and Unified Theories 11-18 Mar 2000, Les Arcs, France: XXXVth Rencontres de Moriond
3. P Bussey (Glasgow), *Inclusive Prompt Photon Production and DVCS at HERA*, Moriond Conference on QCD and High Energy Hadronic Interactions 18-25 Mar 2000, Les Arcs, France: XXXVth Rencontres de Moriond
4. O Ruske (Oxford), *The Soft $\rightarrow$ pQCD Interface Region at HERA*, Moriond Conference on QCD and High Energy Hadronic Interactions 18-25 Mar 2000, Les Arcs, France: XXXVth Rencontres de Moriond
5. G McCance (Glasgow), *Event Shapes and Power Correction Results from HERA*, Moriond Conference on QCD and High Energy Hadronic Interactions 18-25 Mar 2000, Les Arcs, France: XXXVth Rencontres de Moriond
6. P Bussey (Glasgow), *Charmonium production at HERA*, UK Phenomenology Workshop on Heavy Flavour and CP Violation (Durham, 2000)
7. P Bussey (Glasgow), *Open heavy flavour production at HERA*, UK Phenomenology Workshop on Heavy Flavour and CP Violation (Durham,2000)
8. N Brook (Bristol), *QCD at HERA*, Annual Conference of the IoP High Energy Particle Physics Group 11-13 Apr 2000, Edinburgh, Scotland (U.K.): IoP2000

9. E Heaphy (U.C.L.), *Recent Results in High E_T Photoproduction*, Session WG1 Structure functions, 8th International Workshop on Deep Inelastic Scattering and QCD 25-30 Apr 2000, Liverpool, UK: DIS2000
10. J Scott (Bristol), *Structure Functions at low and x and Q^2 at ZEUS*, Session WG2 Tests of QCD, 8th International Workshop on Deep Inelastic Scattering and QCD 25-30 Apr 2000, Liverpool, UK: DIS2000
11. N Brook (Bristol), *Azimuthal Asymmetries in DIS*, Session WG2 Tests of QCD, 8th International Workshop on Deep Inelastic Scattering and QCD 25-30 Apr 2000, Liverpool, UK: DIS2000
12. SW Lee (Glasgow), *Prompt Photons in Photoproduction at HERA*, Session WG2 Tests of QCD, 8th International Workshop on Deep Inelastic Scattering and QCD 25-30 Apr 2000, Liverpool, UK: DIS2000
13. K Long (I.C.), *Future High Q^2 Deep Inelastic Scattering at HERA*, Session WG3 Physics at highest Q^2 and P_t, 8th International Workshop on Deep Inelastic Scattering and QCD 25-30 Apr 2000, Liverpool, UK: DIS2000
14. J Cole (Bristol), *Diffractive D^** , Session WG4 High energy scattering and diffraction, 8th International Workshop on Deep Inelastic Scattering and QCD 25-30 Apr 2000, Liverpool, UK: DIS2000
15. A Doyle (Glasgow), *Structure Functions at High Q^2*, 7th Conference on Intersections between Particle and Nuclear Physics 22-28 May 2000, Quebec, Ontario, Canada: CIPANP2000
16. C Cormack (Rutherford), *Structure Functions at Very High Q^2 from HERA*, 7th Conference on Intersections between Particle and Nuclear Physics 22-28 May 2000, Quebec, Ontario, Canada: CIPANP2000
17. M Sutton (Oxford), *High Pt jets*, 15th High-Energy Physics International Euroconference in Quantum Chromodynamics 6-13th July 2000, Montpellier, France: QCD Euroconference 2000
18. R Tapper (Bristol), *Hadronic final state in Deep Inelastic Scattering at HERA*, IVth Rencontres du Vietnam, International Conference on Physics at Extreme Energies 19-25 Jul 2000, Hanoi, Vietnam: Vietnam2000
19. J Butterworth (U.C.L.), *Dijet production transparencies*, Session PA02: Soft interaction processes XXXth International Conference on High Energy Physics ICHEP2000 27 July-2 August 2000, Osaka, Japan
20. N Brook (Bristol), *Multiplicity studies at HERA*, Session PA03: Hard interaction processes XXXth International Conference on High Energy Physics ICHEP2000 27 July-2 August 2000, Osaka, Japan
21. C Cormack (Rutherford), *Measurement of high-Q^2 Neutral Current cross sections in e-p DIS and a first measurement of xF_3*, Contributed Paper to Session PL-11: Hard Interaction Processes XXXth International Conference on High Energy Physics ICHEP2000 27 July-2 August 2000, Osaka, Japan
22. C Glasman (Glasgow), *Jet substructure*, International Conference on the Structure and Interactions of the Photon including the 13th International Workshop on Photon-Photon Collisions 26-31 August 2000, Ambleside, England: Photon 2000
23. C Glasman (Glasgow), *Virtual photon structure*, International Conference on the Structure and Interactions of the Photon including the 13th International Workshop on Photon-Photon Collisions 26-31 August 2000, Ambleside, England: Photon 2000

24. P Bussey (Glasgow), , International Workshop on Skewed Parton Distribution and Lepton-Nucleon Scattering 11-12 Sep 2000, DESY, Germany: SP2000
25. R Devenish (Oxford), *Results from HERA*, DESY Theory Workshop on CP violation and B physics 26-29 Sep 2000, DESY, Germany:
26. C Foudas (I.C.), *Photon structure*, International Conference on Hadron Structure 2-8 Oct 2000, Stara Lesna, High Tatras Mountains, Slovakia: Hadron Structure'2000
27. M Cooper-Sakar (Oxford), *Low-x and F2*, 30th International Symposium on Multiparticle Dynamics 9-15 Oct 2000, Tihany, Lake Balaton, Hungary: ISMD2000
28. B Foster (Bristol), *Low x Physics*, in "The quark structure of matter" Royal Society of London on May 25th 2000
29. B Foster (Bristol), , seminar at Ohio State 29th March 2000
30. B Foster (Bristol), , seminar at Yale 30th March 2000
31. B Foster (Bristol), , seminar at UC Santa Cruz 3rd April 2000
32. B Foster (Bristol), *Particle Physics over the next 20 years* , OECD Megascience Forum, DESY November 9th. 2000
33. B Foster (Bristol), *To see a world in a grain of sand*, Annual Meeting of the Alexander von Humboldt Stiftung, at Bamberg, Germany, April 6-9, 2000

References

[1] PPARC Frontiers Magazine Jan 2000.

[2] Proceedings of the workshop on 'Future Physics at HERA', eds. G. Ingelman, A de.Roeck and R. Klanner, DESY 1996.

[3] V. Andreev et al., *A Proposal for an Upgrade of the HERA Polarimeters for HERA 2000*, DESY-PRC-99-04.

[4] V. Andreev et al., *POL2000: Status and Plans: An Appendix to the POL2000 Proposal*, DESY-PRC-99-05.

[5] APV25 Users Guide, http://www.te.rl.ac.uk/med/apv25_web/user_guide.html

[6] E. Murer, VI2C, VME I2C Users Manual

[7] M. Morrissey, SEQSI Users Manual

[8] G. Claus, W. Dulinski and A. Lounis, CRN-96-33.

[9] L. Malter, Phys.Rev. 50 (1936), 48.

[10] ZEUS Collaboration, J. Breitweg et al., *ZEUS results on the measurement and phenomenology of F-2 at low x and low Q(2)*, The European Physical Journal C7 (1999) 609-630.

[11] ZEUS Collaboration, J. Breitweg et al., *Measurement of inclusive $D^{*\pm}$ and associated dijet cross sections in photoproduction at HERA.* The European Physical Journal C6 (1999) 67-83

[12] ZEUS Collaboration; J. Breitweg et al., *Measurement of $D^{*\pm}$ production and the charm contribution to F_2 in deep inelastic scattering at HERA*, The European Physical Journal C12 (2000) 35-52

[13] ZEUS Collaboration; J. Breitweg et al., *Angular and Current-Target Correlations in Deep Inelastic Scattering at HERA*, The European Physical Journal C12 (2000) 53-68

[14] ZEUS Collaboration; J. Breitweg et al., *Measurement of the Spin-Density Matrix Elements in Exclusive Electroproduction of ρ^0 Mesons at HERA*, The European Physical Journal C12 (2000) 393-410

[15] ZEUS Collaboration; J. Breitweg et al., *Measurement of high-Q^2 charged-current e^+p deep inelastic scattering cross sections at HERA*, The European Physical Journal C12 (2000) 411-428

[16] ZEUS Collaboration; J. Breitweg et al., *Measurement of diffractive photoproduction of vector mesons at large momentum transfer at HERA*, The European Physical Journal C14 (2000) 2, 213-238

[17] ZEUS Collaboration; J. Breitweg et al., *Search for Contact Interactions in Deep Inelastic $e^+p \to e^+X$ Scattering at HERA*, The European Physical Journal C14 (2000) 239-254

[18] ZEUS Collaboration; J. Breitweg et al., *Measurement of inclusive prompt photon photoproduction at HERA*, Physics Letters B 472 (2000) 175-188

[19] ZEUS Collaboration; J. Breitweg et al., *Measurement of the $E^2_{T,jet}/Q^2$ dependence of forward jet production at HERA*, Physics Letters B474 (2000) 223-233

[20] ZEUS Collaboration; J. Breitweg et al., *Search for resonances decaying to e^+-jet in e^+p interactions at HERA*, The European Physical Journal C16 (2000) 253-267

[21] ZEUS Collaboration; J. Breitweg et al., *The Q^2 dependence of dijet cross sections in γ-p interactions at HERA*, Physics Letters B479 (2000) 37-52

[22] ZEUS Collaboration; J. Breitweg et al., *Measurement of Azimuthal Asymmetries in Deep Inelastic Scattering*, Physics Letters B481 (2000) 199-212

[23] ZEUS Collaboration; J. Breitweg et al., *Measurement of Inclusive $D_s^{\pm}$ Photoproduction at HERA*, Physics Letters B481 (2000) 213-227

[24] ZEUS Collaboration; J. Breitweg et al., *Measurement of the Proton Structure Function F_2 at Very Low Q^2 at HERA*, Physics Letters B487 (2000) 53-73

[25] ZEUS Collaboration; J. Breitweg et al., *Measurement of exclusive ω electroproduction at HERA*, Physics Letters B487 (2000) 273-288

[26] ZEUS Collaboration; J. Breitweg et al., *A search for resonance decays to anti-nu jet in e+ p scattering at HERA* (Sep 2000), accepted by Phys. Rev. D

[27] ZEUS Collaboration; J. Breitweg et al., *Measurement of dijet cross sections for events with a leading neutron in photoproduction at HERA* (Oct 2000), accepted by Nuclear Physics B

[28] ZEUS Collaboration; J. Breitweg et al., *Measurement of open beauty production in photoproduction at HERA* (Nov 2000), accepted by The European Physical Journal C

[29] J. Breitweg et al., Eur. Phys. J. C 12 (2000) 411.

[30] H.L. Lai et al., Phys. Rev. D 55 (1997) 1280.

[31] E.A.Heaphy, *Three-jet Production at HERA*, Durham Workshop on Collider Physics, Sept. 1999.

[32] ZEUS Collaboration, J. Breitweg et al., Phys. Lett. B 443 (1998) 394-408.

[33] R. Waugh, Glasgow University Ph.D. Thesis (1999); G. McCance, "Event Shapes at HERA", Moriond Proceedings (in preparation).

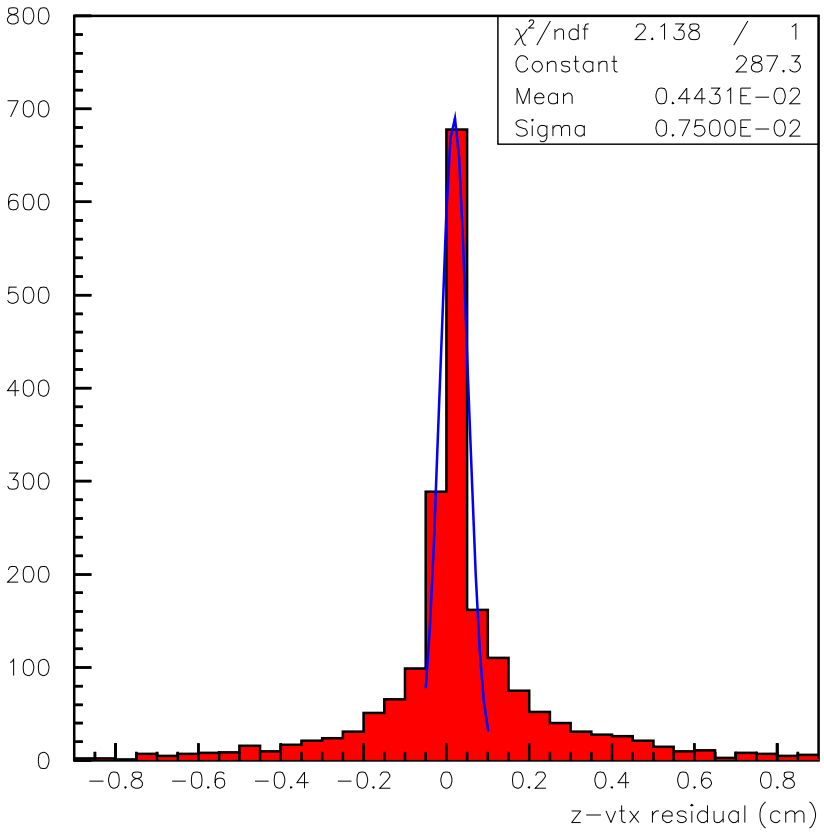

Figure 1: The z-vertex resolution of the GTT algorithm using CTD stereo and MVD information (cf the $\sim 100\,\mu$m resolution with $\sim 9\,$cm for the cuttent CTD-SLT.)

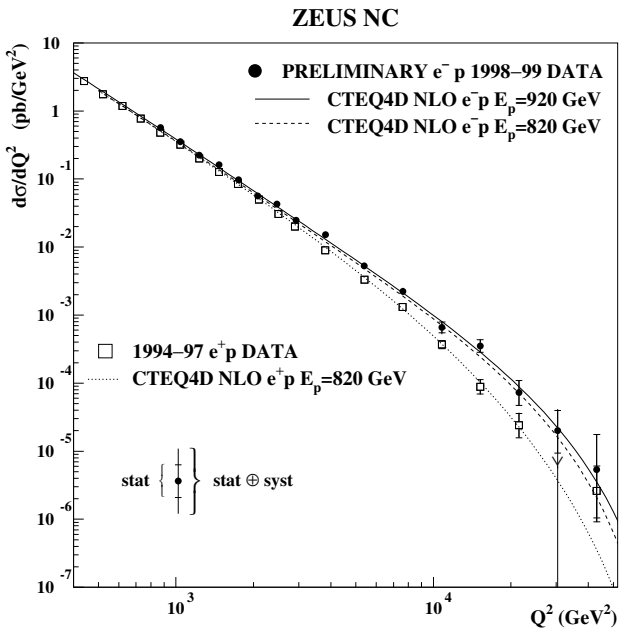

Figure 2: Shown is the single differential e^+p and e^-p $d\sigma/dQ^2$ cross section with the Standard Model predictions from CTEQ4D in the solid line and MRST in the dashed line. For high values of $Q^2 > 3000\,\mathrm{GeV}^2$ the e^-p cross section is seen to lie above the e^+p cross section.

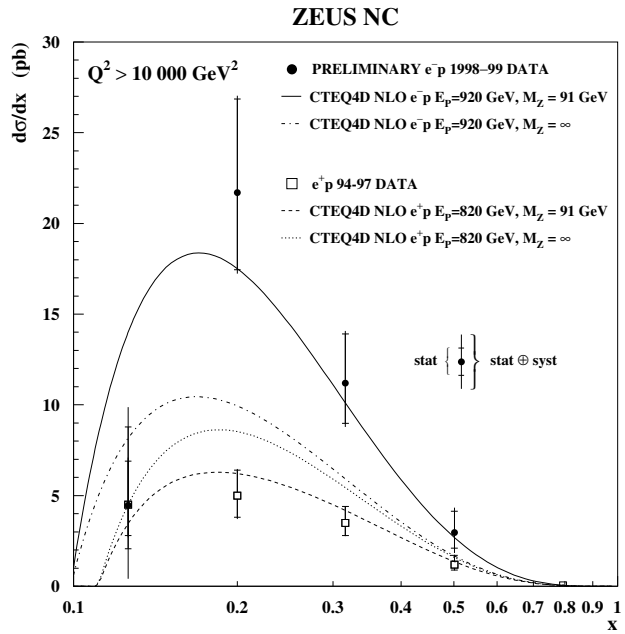

Figure 3: Shown is the single differential e^+p and e^-p $d\sigma/dx$ cross section for $Q^2 > 10\,000\,\mathrm{GeV}^2$ with the Standard Model predictions from CTEQ4D in the solid line and MRST in the dashed line. It can be seen that the e^-p has a larger cross section than the e^+p data.

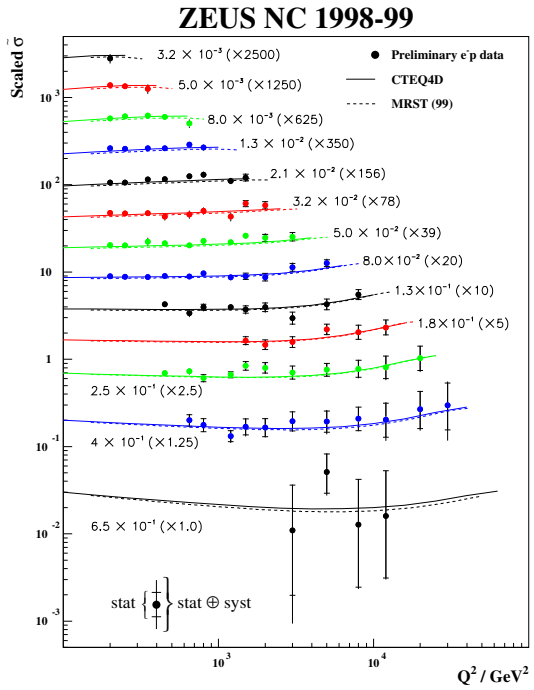

Figure 4: Shown is the reduced e^+p and e^-p cross section with the Standard Model predictions from CTEQ4D in the solid line and MRST in the dashed line. For high values of $x > 0.18$ the e^-p data is seen to rise at high values of Q^2, this is as opposed to the e^+p data which turns down at large values of Q^2.

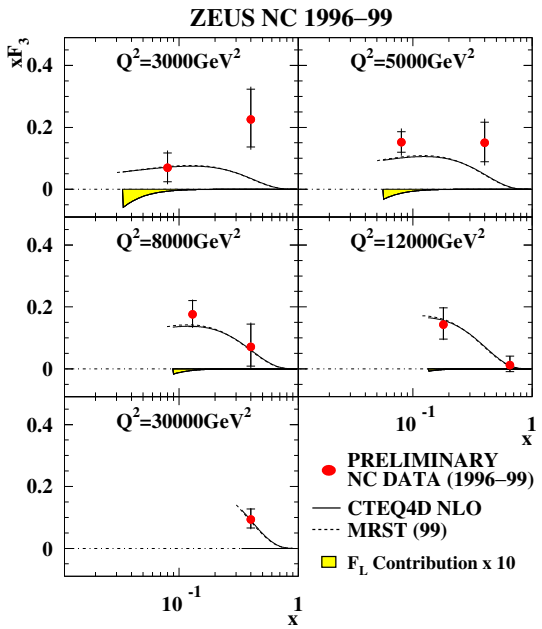

Figure 5: Shown is the extraction of xF_3 at fixed Q^2 as a function of x with the Standard Model predictions from CTEQ4D in the solid line and MRST in the dashed line. The data is well described by both MRST and CTEQ4D predictions

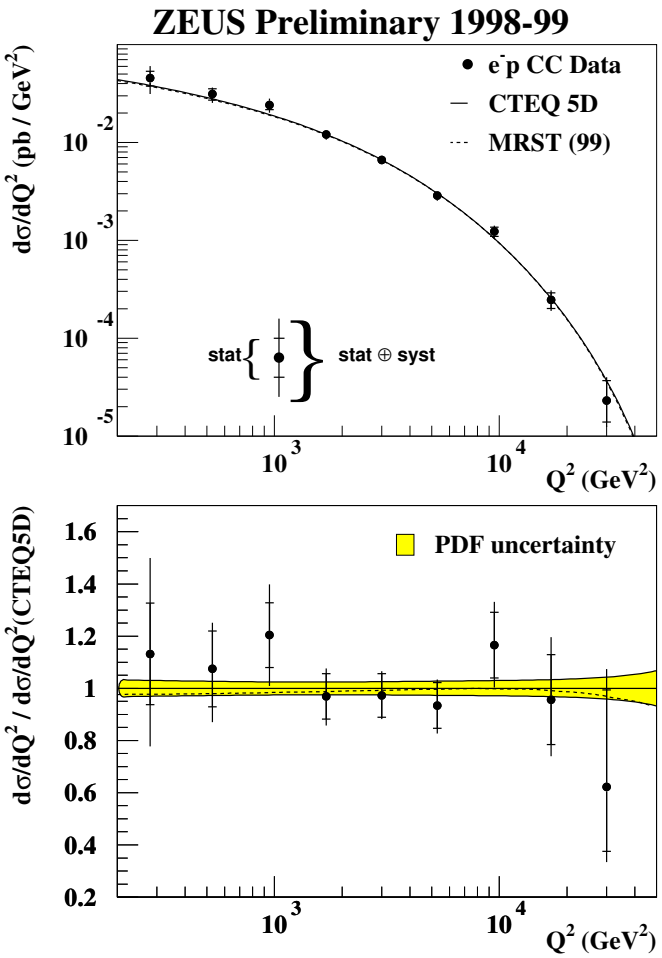

Figure 6: (a) The e^-p CC DIS Born cross section, $d\sigma/dQ^2$, for data (solid points) and the Standard Model expectation evaluated using the CTEQ5D and MRST (99) PDFs. (b) The ratio of the measured cross section, $d\sigma/dQ^2$, to the Standard Model expectation evaluated using the CTEQ5D PDFs. The statistical errors are indicated by the inner error bars (delimited by horizontal lines), while the full error bars show the total error obtained by adding the statistical and systematic contributions in quadrature. The shaded band shows the uncertainties associated with the PDFs.

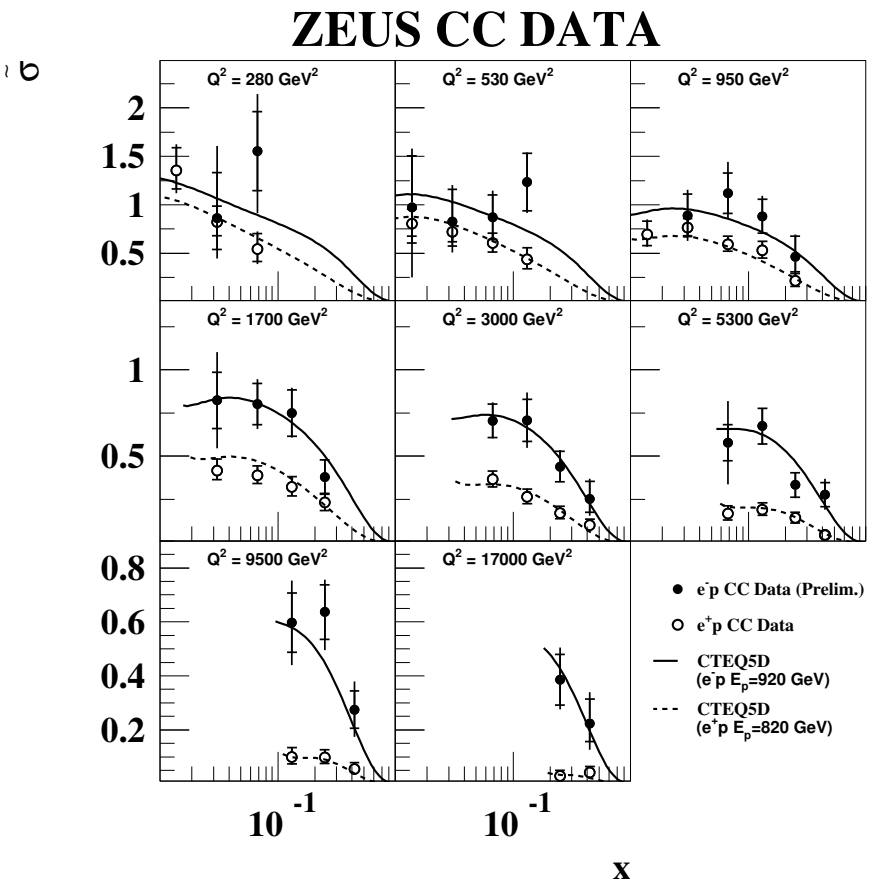

Figure 7: The reduced cross section, $\tilde{\sigma}$, as a function of x, for different fixed values of Q^2. The filled and open dots represent the e^-p and e^+p data respectively, while the expectations of the Standard Model evaluated using the CTEQ5D PDFs are shown as the solid and dotted lines.

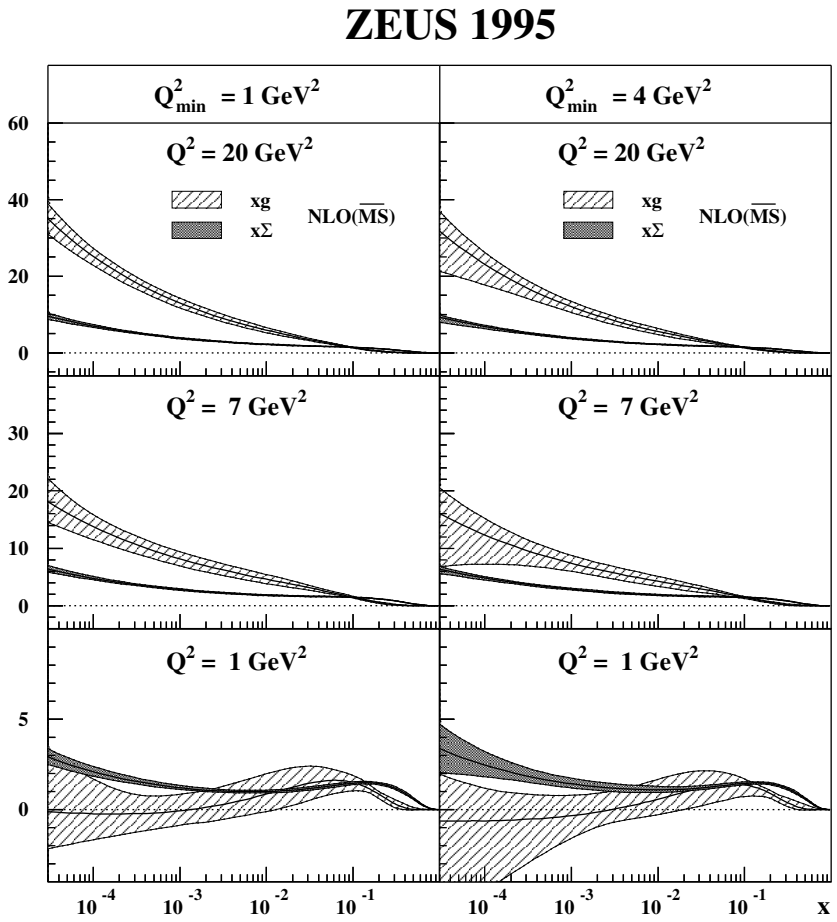

Figure 8: The quark singlet momentum distribution, $x\Sigma$ (shaded), and the gluon momentum distribution, $xg(x)$ (hatched), as functions of x at fixed values of $Q^2 = 1$, 7 and 20 GeV^2 from the ZEUS QCD fit. The error bands correspond to the quadratic sum of all error sources considered for each parton density. The three left-hand (right-hand) plots show the results from the standard fit including F_2 data with $Q^2 > 1$ GeV^2 (4 GeV^2).

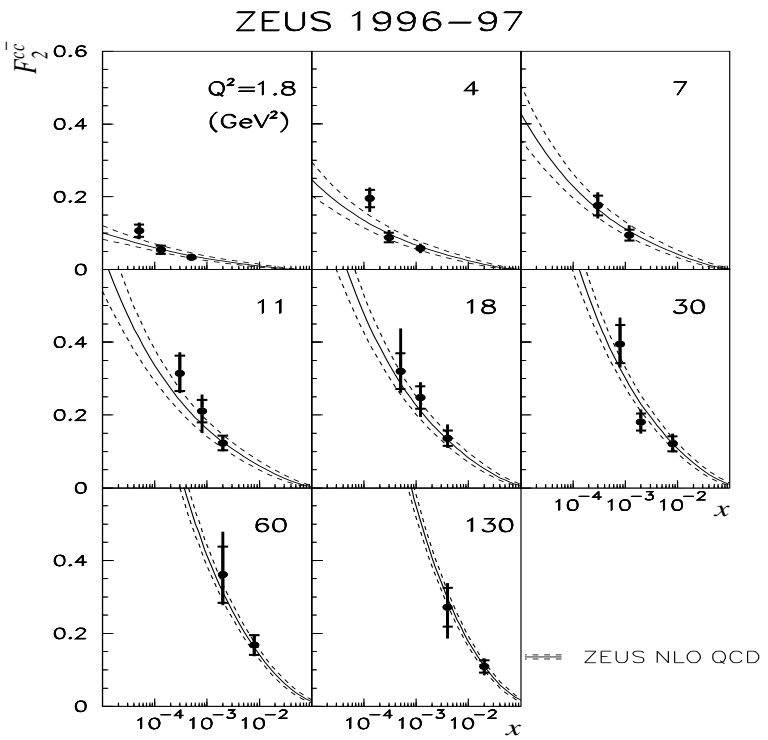

Figure 9: F_2^c as a function of x at fixed Q^2.

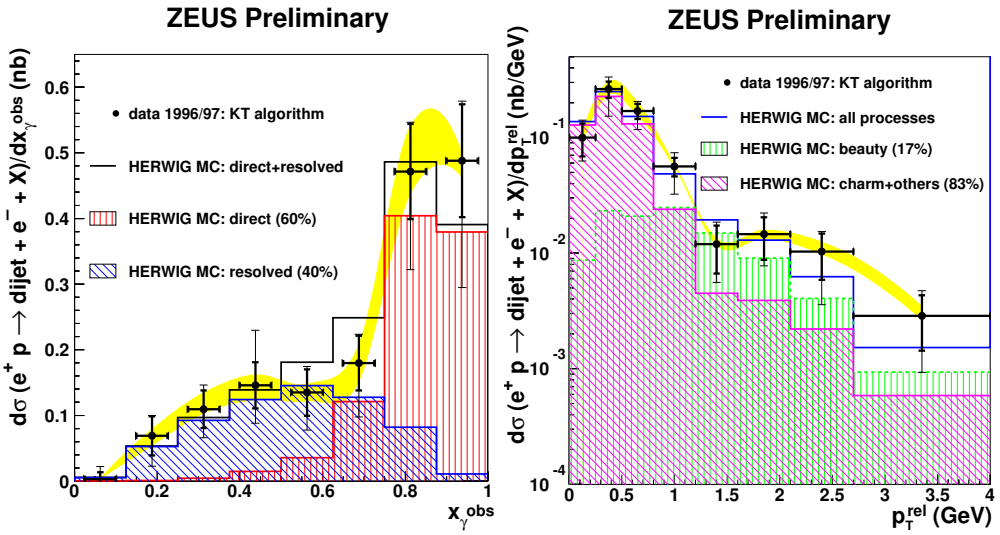

Figure 10: (a) The x_γ^{OBS} distribution for heavy flavour decays tagged with an electron, confirming the presence of a resolved component. (b) The transverse momentum of the electron relative to the jet axis, showing the presence of beauty quarks.

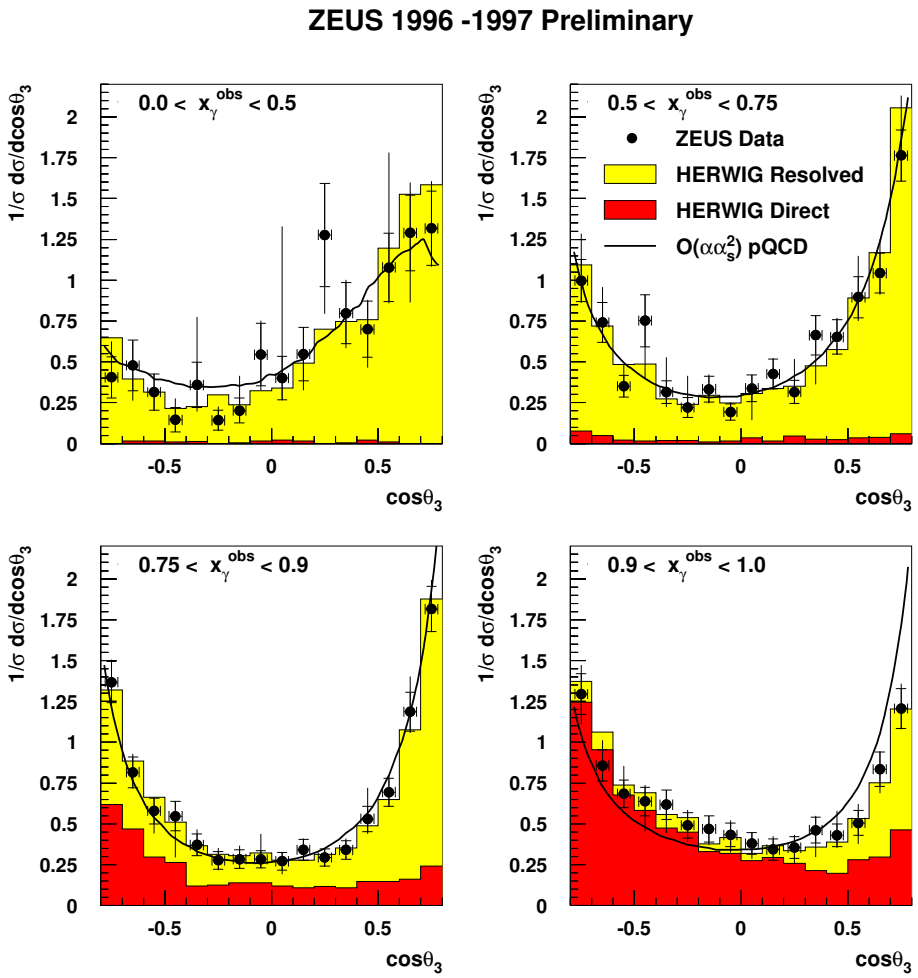

Figure 11: ZEUS preliminary three jet cross sections. LO resolved photon processes are shown by light shading, and LO direct by dark shading.

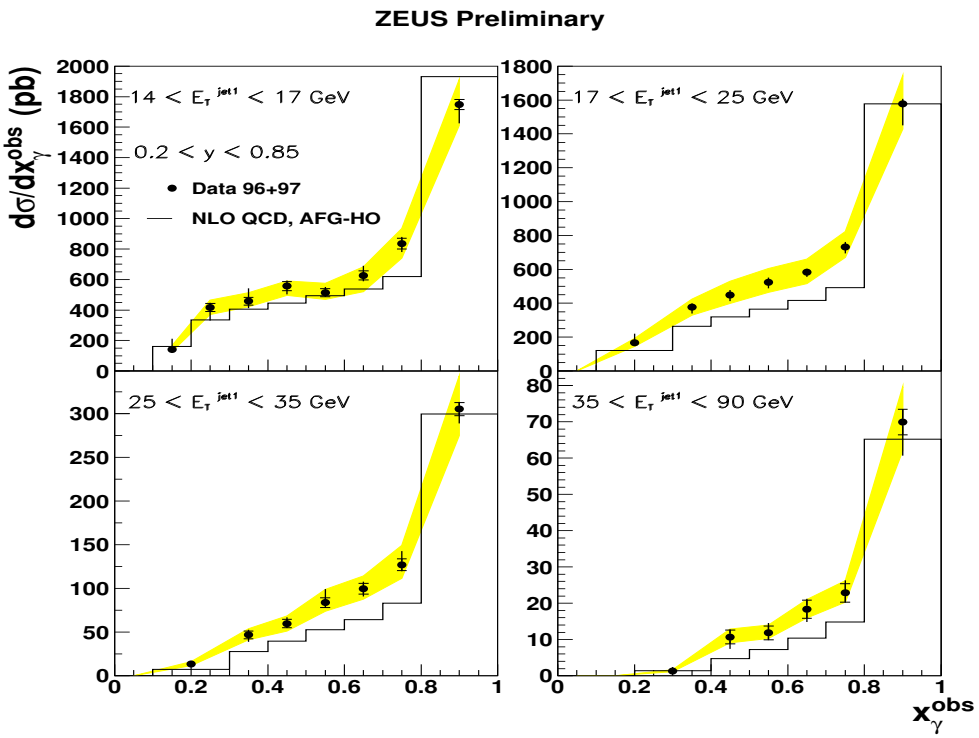

Figure 12: ZEUS preliminary jet cross sections compared to the NLO QCD calculation of Frixione and Ridolfi. The shaded area indicates the hadronic energy-scale uncertainty.

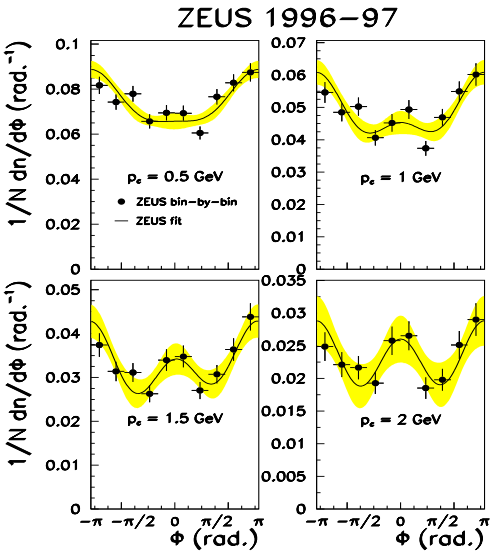

Figure 13: The differential ϕ distributions obtained for four values of the p_T cut, p_c, in the hadronic centre-of-mass frame in the kinematic region $0.01 < x < 0.1$ and $0.2 < y < 0.8$ for charged hadrons with $0.2 < z_h < 1.0$. The full line (with accompanying statistical error band) is the result obtained from the main analysis using the unfolding technique. The data points were corrected using a bin-by-bin procedure (only statistical errors are shown).

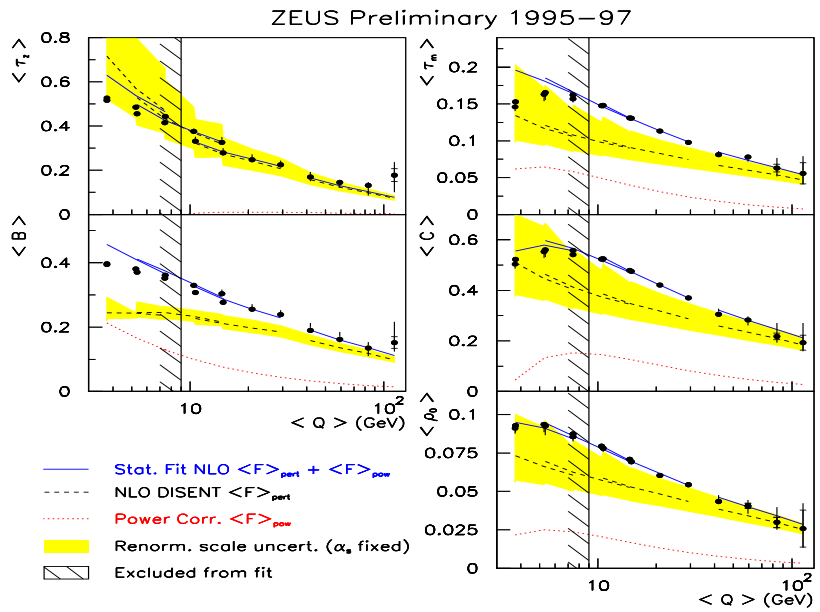

Figure 14: ZEUS preliminary mean event shape variables versus Q compared to two-parameter fits using the NLO calculation plus power correction approach described in the text. The shaded region represents the renormalisation scale uncertainty where $Q/2 < \mu_R < 2Q$, with α_S fixed to the fitted value.

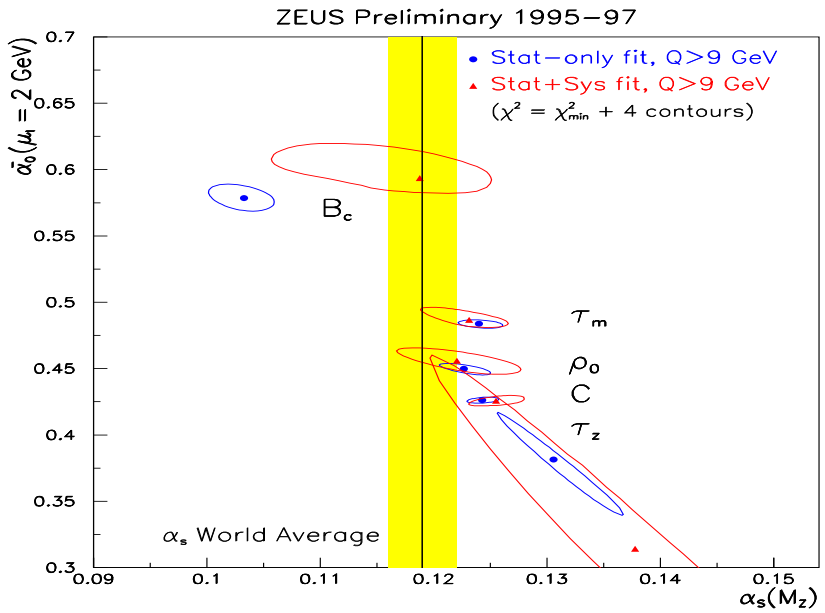

Figure 15: ZEUS preliminary contour plot of two-parameter fits of $\overline{\alpha}_0(\mu_I)$ and $\alpha_s(M_Z)$ to mean event shape variables. 2σ stat and stat$\oplus$sys contours for τ, B, τ_C, ρ and C parameters are indicated.

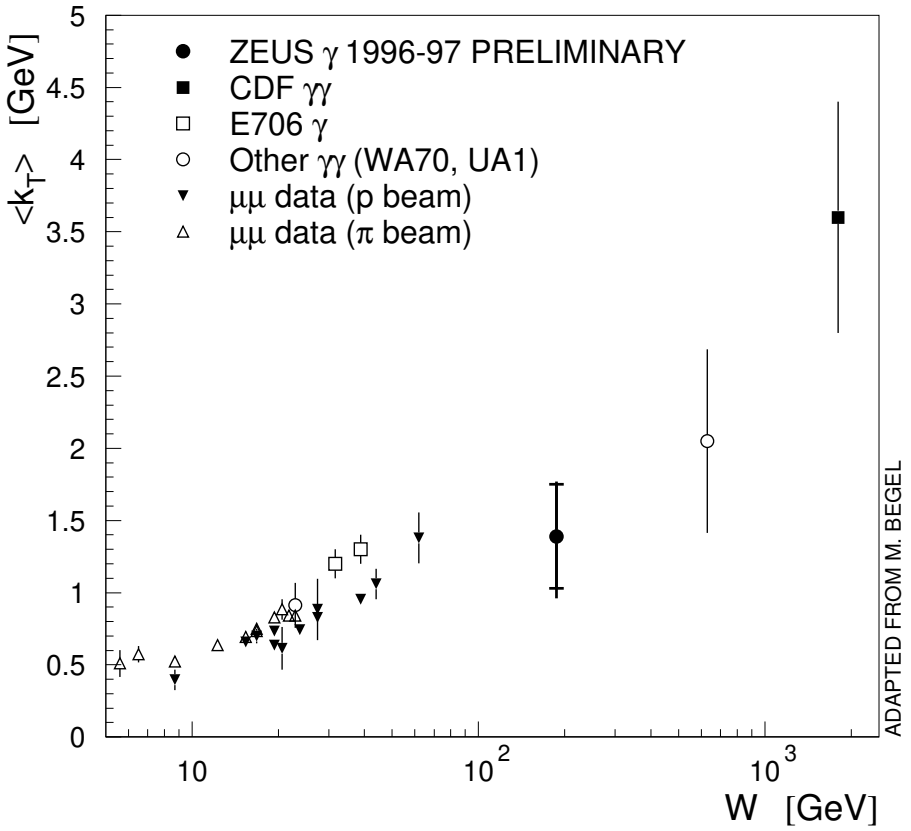

Figure 16: Effective transverse momentum of quarks within a proton, as they take part in direct photoproduction of a high transverse momentum prompt photon and a jet.